0026-895X/04/6604-855–863$20.00
MOLECULAR PHARMACOLOGY
Copyright © 2004 The American Society for Pharmacology and Experimental Therapeutics
Mol Pharmacol 66:855–863, 2004

Vol. 66, No. 4
1719/1176678
Printed in U.S.A.

Stannin, A Protein That Localizes to the Mitochondria and Sensitizes NIH-3T3 Cells to Trimethyltin and Dimethyltin Toxicity

Collin E. Davidson, Brian E. Reese, Melvin L. Billingsley, Jong K. Yun

Department of Pharmacology (C.E.D., B.E.R., M.L.B., J.K.Y.) and Jake Gittlen Cancer Research Institute (J.K.Y.), Pennsylvania State University College of Medicine, Hershey, Pennsylvania

Received April 22, 2004; accepted July 15, 2004

ABSTRACT

Stannin (Snn) is a highly conserved, 88-amino acid protein that may mediate the selective toxicity of organotins. Snn is localized in tissues with known sensitivity to trimethyltin (TMT), including the central nervous system, immune system, spleen, kidney and lung. Cells in culture that do not express Snn show considerable resistance to TMT toxicity. In vitro, Snn peptide can bind TMT in a 1:1 ratio and can de-alkylate TMT to dimethyltin (DMT). We now show that transfection with Snn sensitized TMT-resistant NIH-3T3 mouse fibroblasts to both TMT and DMT cytotoxicity. Triple label confocal microscopy of Snn-transfected cells and Percoll gradient purification of mitochondria showed Snn localized to the mitochondria and other membrane structures. The mitochondrial localization of Snn, coupled with its ability to bind and dealkylate organotin compounds, indicates a possible mechanism by which selective alkyltin toxicity might be mediated.

Alkyltins have been used as heat stabilizers in polyvinylchloride tubing, curing agents for rubber production, disinfectants in hospitals, and as biocides (Snoeij et al., 1987; Aschner and Aschner, 1992). Toxicity from accidental exposure to alkyltins has lead to considerable research characterizing their selective toxicity in mammals (Ross et al., 1981; Snoeij et al., 1987; Boyer, 1989).

Trimethyltin (TMT) is a potent toxicant that selectively kills cells in the central nervous system, immune system, spleen, lung, and kidney (Brown et al., 1979; Philbert et al., 2000; Snoeij et al., 1985). The 'TMT syndrome' had been used to characterize the phenotype observed after intoxication in rodents; abnormalities after intoxication include spontaneous seizures, self-mutilation, vocalizations, whole-body tremors, and hyper-reactivity to touch (Dyer et al., 1982). Human exposure results in pathology closely resembling that of other mammals (Ross et al., 1981; Feldman et al., 1993). TMT intoxication resulted in phenotypic changes indicative of apoptotic cell death, which includes chromatin condensation, nuclear fragmentation, mitochondrial dysfunction, reactive oxygen species production, membrane blebbing, and caspase activation (Brown et al., 1979; Stine et al., 1988; LeBel et al., 1990; Geloso et al., 2002; Jenkins and Barone, 2004). Within the central nervous system, TMT selectively destroyed neurons located in the neocortex, amygdala, and olfactory tubercle, but its most striking effects were in the hippocampal formation (Brown et al., 1979; Balaban et al., 1988; Thompson et al., 1996).

Subtractive hybridization of TMT-treated versus untreated control rat brain was used to isolate the stannin (Snn) gene product. (Krady et al., 1990). In situ hybridization of adult rat brain for Snn mRNA demonstrated that Snn was expressed in the hippocampal formation, neocortex, and other limbic structures, correlating with areas sensitive to TMT (Dejneka et al., 1997). Northern blots of rat tissue mRNA revealed that Snn was expressed in spleen, brain, kidney, and lung, but was below detection levels in liver, heart, skeletal muscle, and testes (Dejneka et al., 1997). Examination of TMT toxicity in cultured cells showed that cells expressing Snn were considerably more sensitive to TMT (Thompson et al., 1996). On the other hand, preincubation with antisense oligonucleotides directed against Snn mRNA protected primary neurons in culture from TMT toxicity (Thompson et al., 1996).

Molecular characterization of Snn predicted an 88 amino

This work was supported by United States Public Health Service grant ES05540 (to M.L.B.).
Article, publication date, and citation information can be found at http://molpharm.aspetjournals.org.
doi:10.1124/mol.104.001719.

ABBREVIATIONS: TMT, trimethyltin; DMT, dimethyltin; GRP, gastrin-releasing peptide; HRP, horseradish peroxidase; FITC, fluorescein isothiocyanate; GFP, green fluorescent protein; PBS, phosphate-buffered saline; DAPI, 4′,6-diamidino-2-phenylindole; PAGE, polyacrylamide gel electrophoresis; TBS, Tris-buffered saline; HEK, human embryonic kidney.

acid protein expressed only in vertebrates (Toggas et al., 1992). Furthermore, this protein exhibits a high level of conservation; the rat, mouse, and human Snn differ by only two amino acids in the carboxyl terminus. Lower vertebrates, such as frog (*Xenopus laevis*) and Zebrafish (*Danio rerio*), share 89 and 91% similarity with the human protein sequence, respectively. Structural analysis using several algorithms predicts an amino-terminal transmembrane domain followed by a hydrophilic loop (Dejneka et al., 1997). The carboxyl-terminal domain seems to be a membrane-associated random coil (Buck et al., 2003).

Direct association of Snn with alkyltins has been shown using a peptide corresponding to amino acids 29–37 of Snn (Buck et al., 2003). These nine amino acids located within the predicted cytoplasmic loop contain two cysteines (amino acids 32 and 34), forming a vicinal thiol. Vicinal thiols are implicated in heavy metal binding, suggesting a possible binding domain for TMT. Electrospray ionization mass spectrometry of the Snn peptide in the presence of trisubstituted alkyltins showed that Snn bound to and dealkylated TMT to dimethyltin (DMT). Snn remained in association with DMT in a [1:1] ratio after the methyl group was removed (Buck et al., 2003).

Although TMT toxicity has been studied in depth, molecular characterization of DMT toxicity and its intracellular targets are not as well characterized. DMT is used as a heat stabilizer for polyvinylchloride tubing and may contaminate drinking water supplies (Braman and Tompkins, 1979; Sadiki and Williams, 1996). In rats, DMT can be absorbed through the digestive tract and passed through the placenta to the pup, where it accumulates in the fetal blood and brain (Noland et al., 1983). DMT is less toxic in vitro and in vivo compared with trisubstituted organotins (Mushak et al., 1982; Komulainen and Bondy, 1987); this reduced toxicity may be because of its lower hydrophobicity and inability to readily cross the plasma membrane. TMT exposure can result in mitochondrial dysfunction and increased reactive oxygen species, although its specific target(s) remain unclear (Stine et al., 1988; LeBel et al., 1990).

We now demonstrate that Snn is a mitochondrial target for TMT and DMT toxicity. Subcellular localization of Snn in mitochondria and other organelles indicates a possible common link to alkyltin toxicity. Furthermore, we show that Snn transfection into NIH-3T3 fibroblasts sensitized these cells to the toxic effects of TMT and to a lesser extent, DMT.

Materials and Methods

Materials. The empty vector pcDNA3.1, T4 DNA ligase, XhoI and HinDIII endonucleases were obtained from Invitrogen (Carlsbad, CA). Subcloning efficiency DH5-α *Escherichia coli* were purchased from Stratagene (La Jolla, CA). Cell culture reagents were obtained from Invitrogen, including 0.25% Trypsin, EDTA, and antibiotic/antimitotic mixture and high-glucose Dulbecco's modified Eagle's medium containing sodium pyruvate and pyridoxine hydrochloride. LipofectAMINE2000 and Opti-MEM I containing HEPES buffer, sodium bicarbonate and L-glutamine were also purchased from Invitrogen. Trimethyltin chloride and dimethyltin dichloride were a gift from Dr. James O'Callahan, National Institute for Occupational Safety and Health/Centers for Disease Control and Prevention (Morgantown, WV).

Antibodies. Mouse anti-FLAG (M2 monoclonal) and rabbit anti-FLAG (polyclonal) were purchased from Sigma (St. Louis, MO). Rabbit anti-active caspase-3 and rabbit anti-caspase-9 were purchased from Cell Signaling Technology (Beverly, MA). Mouse anti-α-spectrin was obtained from Chemicon (Temecula, CA), and rabbit anti-Elk-1, goat anti-GRP-75, goat anti-GRP-78, horseradish peroxidase (HRP)-conjugated goat anti-mouse, HRP-conjugated goat anti-rabbit, and HRP-conjugated rabbit anti-goat were obtained from Santa Cruz Biotechnologies (Santa Cruz, CA). FITC-conjugated donkey anti-goat and Texas Red-conjugated donkey anti-rabbit were purchased from Jackson Immunoresearch Laboratories (West Grove, PA).

Subcloning. The Snn open reading frame, with the addition of the amino-terminal FLAG-tag epitope, was subcloned into pcDNA3.1 using the full Snn cDNA sequence in pBluescript (Dejneka et al., 1997) as a template. PCR primers were constructed containing the FLAG-tag epitope sequence added to the amino terminal of Snn (N-terminal primer: GGG CTC GAG ATG GAC TAC AAG GAC TAC AAG GAC GAC GAC GAC AAG ATG TCT ATT ATG GAC CAC AGC; C-terminal primer: GGG AAG CTT TCA GCC ATG CAC TTC CGG G). The pcDNA3.1 vector and the Snn-FLAG insert were digested using XhoI and HinDIII restriction endonucleases. Snn-FLAG was ligated into pcDNA3.1 using T4 DNA ligase and subsequently transformed into DH5α *E. coli*. Transformed DH5α were plated onto agar plates using ampicillin (50 μg/ml) as a selection marker. Plates were incubated at 37°C for 12 h. Colonies were transferred to Luria-Bertani media containing ampicillin at 50 μg/ml. Plasmid DNA for Snn-FLAG-pcDNA3.1 was extracted (plasmid miniprep kit; QIAGEN, Valencia, CA), and positive clones were sequence verified. Green fluorescent protein (GFP)-pcDNA3.1 was constructed with a carboxyl-terminal FLAG-tag using the same method and restriction sites (N-terminal primer: GGG AAG CTT ACC ATG GTG AGC AAG GGC G; C-terminal primer: GGG CTC GAG TCA CTT GTC GTC GTC GTC CTT GTA GTC CTT GTA CAG CTC GTC CAT GC).

Cell Culture. NIH-3T3 mouse fibroblasts (American Type Culture Collection, Manassas, VA) were cultured in high-glucose Dulbecco's modified Eagle's medium with 10% heat-inactivated Cool Calf-2 Serum (Sigma) with antibiotic/antimitotic mixture. For subculturing, cells were plated into 75-mm^2 poly-D-lysine–coated flasks (Corning Glassworks, Corning, NY), and maintained at 37°C with 5% CO_2.

Transient Transfection. NIH-3T3 cells were plated at 3.0×10^5 cells per 25-mm^2 flask and allowed to grow for 24 h at 37°C. Six microliters of LipofectAMINE 2000 and 4.8 μg of either Snn-FLAG-pcDNA3.1, GFP-FLAG-pcDNA3.1, or vehicle was incubated with 200 μl of Opti-MEM for 20 min at 24°C. This mixture was then added to the cells and incubated for a total of 24 h. Average transfection efficiency was measured at 25 to 30%, calculated by the expression of GFP after 24 h. Pictures were taken using the Nikon Eclipse TE2000-S microscope and a FITC filter at 100× magnification. The number of FITC-fluorescent cells was counted as a function of the total cells within the observed field.

Immunofluorescent Laser-Scanning Confocal Microscopy. Cells were transfected with Snn-FLAG-pcDNA3.1 and allowed to incubate at 37°C for 24 h. Cells were washed three times with phosphate-buffered saline (PBS). Cells were fixed with 4.0% paraformaldehyde for 5 min, washed three times with PBS, then permeabilized with 0.1% Triton X-100 in PBS for 2 min. The rabbit polyclonal anti-FLAG, and goat polyclonal anti-GRP-75 antibodies were then added (1:200 dilution) and incubated at 24°C for 1 h. Cells were washed three times with PBS and then incubated for 20 min with normal donkey serum (1:50). The Texas Red-conjugated donkey anti-rabbit and FITC-conjugated donkey anti-goat antibodies were added (1:250 dilution) and incubated at room temperature for 1 h. Nuclear staining using 4′,6-diamidino-2-phenylindole (DAPI) was performed after immunocytochemistry. Cells were washed three times with PBS and incubated with 3.0 μM DAPI stain for 5 min. Cells were rinsed three times with PBS and mounted with the use of Gel-Mount mounting media (Fisher Scientific, Pittsburgh, PA). Immunofluorescence was visualized using the Leica DMI RE2 laser-scanning con-

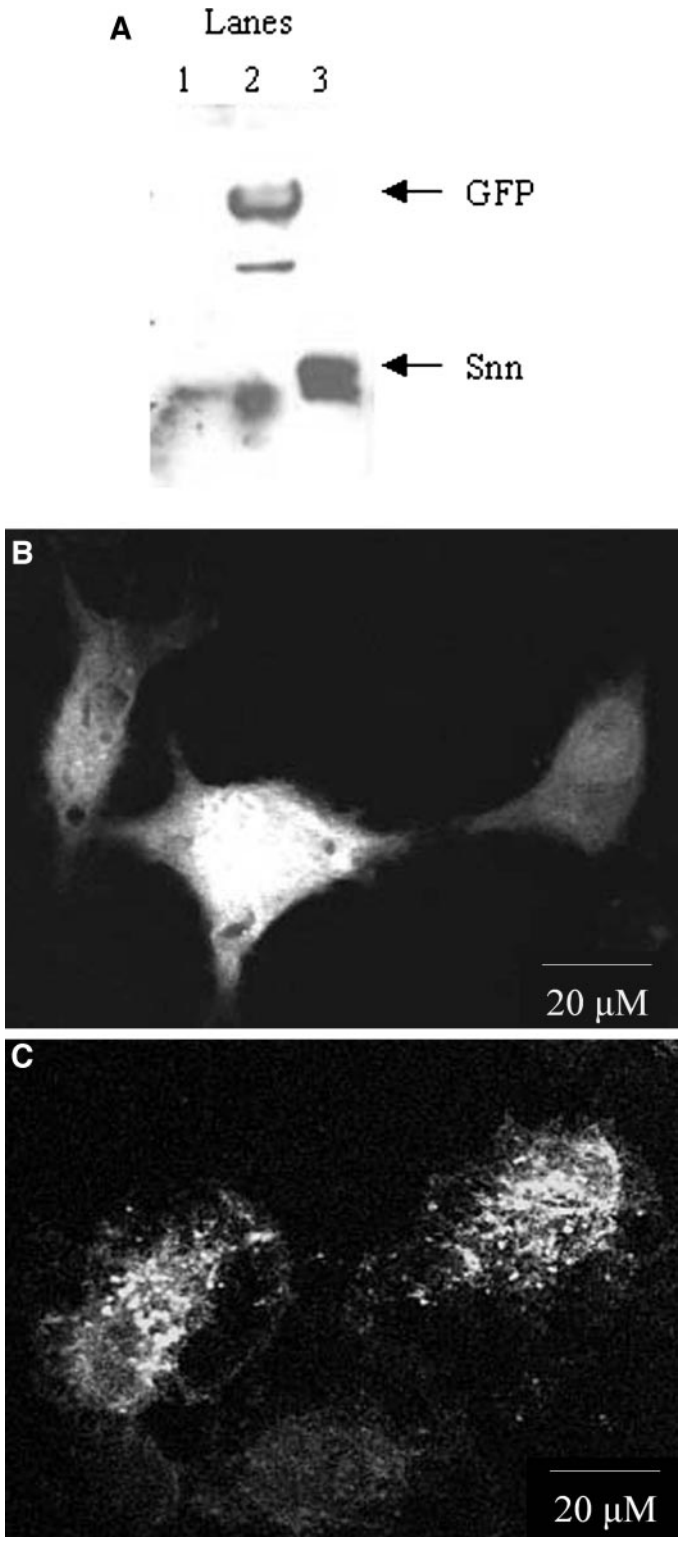

Fig. 1. Stannin expression in NIH-3T3 cells. Cells were transfected with either GFP-FLAG-pcDNA3.1, Snn-FLAG-pcDNA3.1, or with vehicle control. After a 24-h incubation, cells were harvested and used for Western blots or confocal microscopy analysis for anti-FLAG immunoreactivity. A, Western blot analysis for anti-FLAG immunoreactivity. Note that immunoreactivity is observed for both Snn and GFP using the anti-FLAG antibody; 20 μg of total protein was loaded in each lane. Lanes: 1, nontransfection; 2, GFP-FLAG-pcDNA3.1 transfection; 3, Snn-FLAG-pcDNA3.1 transfection. B, laser scanning immunofluorescent confocal micrographs of anti-FLAG immunoreactivity. GFP exhibited diffuse staining equally distributed throughout the cytosol, whereas Snn exhibited punctate intracellular staining.

focal microscope (Leica, Wetzlar, Germany) in the Penn State Confocal Microscopy Facility. Triple emission micrographs were taken; DAPI, FITC, and Texas Red excitation was accomplished using lasers at 405, 488, and 514 nm, and emission was measured at 420 to 480 nm, 500 to 580 nm, and 610 to 670 nm, respectively. All pictures were taken using a 10× eyepiece, 63× objective, and either 2.5× or 4× fine focus zoom to achieve magnifications of 1600× and 2500×, respectively.

Subcellular Fractionation by Differential Centrifugation. NIH-3T3 cells were plated at 1.5×10^6 cells per 75-mm^2 flask and incubated at 37°C for 24 h. Cells were then transfected using methods described above. A total of 14.4 μg of DNA and 18.0 μl of LipofectAMINE 2000 was used per 75-mm^2 flask. After a 24-h incubation, cells were trypsinized and resuspended in 500 μl of homogenization buffer (20 mM HEPES-NaOH, pH 7.2, 0.25 M sucrose, 1.0 mM $MgCl_2$, 1.0 mM EDTA, and mammalian protease inhibitor cocktail [1:50; Sigma]) Cells were incubated for 5 min on ice and sonicated three times for 5 s each. Cells were centrifuged at 1000 rpm (3000*g*) in an Eppendorf tabletop microcentrifuge; the pellet was labeled P1. The supernatant was transferred to a new tube and centrifuged at 20,000 rpm (~33,000*g*) using a TLA100.3 rotor in a Beckman Coulter Ultracentrifuge; this pellet was labeled P2. The supernatant was transferred to a new tube and centrifuged at 55,000 rpm (~100,000*g*), using same rotor and ultracentrifuge; this pellet was labeled P3, and the supernatant was labeled S3. Pellets were then resuspended in lysis buffer containing: 20 mM Tris, pH 7.5, 150 mM NaCl, 1.0 mM EDTA, 1.0 mM EGTA, 1.0% Triton X-100, 2.5 mM sodium pyrophosphate, 1 mM β-glycerolphosphate, 1 mM Na_3VO_4, and [1:50] mammalian protease inhibitor cocktail. Ten micrograms of total protein was used for Western blot analysis.

Percoll Gradient Purification of Mitochondria. NIH-3T3 cells were plated at 1.5×10^6 cells per 75-mm^2 flask and incubated at 37°C for 24 h. Cells were transfected as described above. Cells were then incubated for 24 h, trypsinized, and resuspended in 500 μl of homogenization buffer (10 mM HEPES-NaOH, pH 7.5, 0.25 M sucrose, 1.0 mM dithiothreitol, and 1:50 mammalian protease inhibitor cocktail). Cells were incubated on ice for 10 min and homogenized by 30 strokes with a Teflon Dounce homogenizer. The mixture was then centrifuged for 10 min at 1000 rpm (3000*g*) in an Eppendorf tabletop microcentrifuge. The supernatant was transferred to a new tube and centrifuged for 10 min at 14,000 rpm (27,000*g*). The P2 pellet was then resuspended in 500 μl of mitochondrial isolation buffer (0.25 M mannitol, 25 mM HEPES-NaOH, pH 7.5, 0.5 mM EGTA, and 1:50 mammalian protease inhibitor cocktail). This mixture was loaded on top of 7 ml of mitochondrial isolation buffer

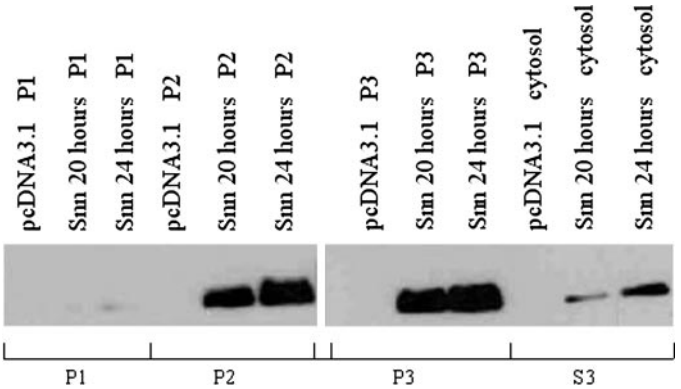

Fig. 2. Subcellular localization of stannin by differential centrifugation fractionation. NIH-3T3 cells were transfected with Snn-FLAG-pcDNA3.1, incubated for 24 h, and subcellular fractions were collected. Twenty micrograms of total protein was used in Western blots. The denotation corresponds to these fractions: P1, 3000*g* fraction; P2, 22,000*g* fraction; P3, 100,000*g* fraction, and S3, cytosol. Snn-FLAG immunoreactivity was detected in the P2 and P3 fractions, with some present in the S3 fraction. The P1 fraction was devoid of Snn-FLAG immunoreactivity.

containing 30% Percoll (Sigma). The mixture was then centrifuged for 30 min at 27,000 rpm (95,000*g*; 4°C) using an SW-40Ti rotor in a Beckman Coulter Ultracentrifuge. Fractions taken include 1) the top 1.5 ml of Percoll gradient, 2) the dense band approximately 40% through the Percoll gradient, and 3) the membrane collected at the bottom of the Percoll gradient (resuspended in 100 μl of lysis buffer). Twenty-five microliters of total lysate was used for Western blot analysis.

SDS-PAGE and Western Blot Analysis. After transient transfection, cells were trypsinized (0.25% trypsin; Invitrogen) and resus-

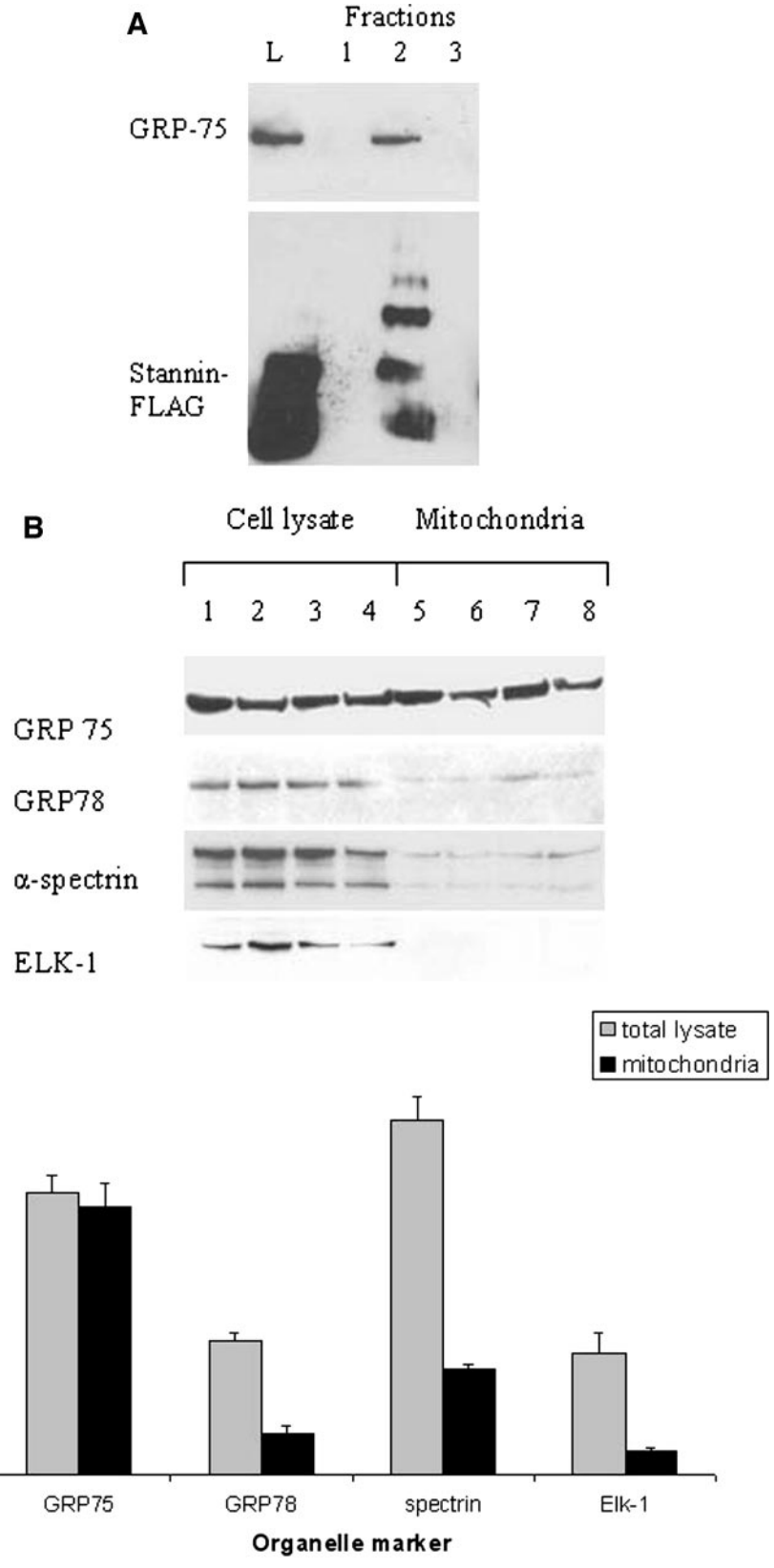

Fig. 3. Percoll gradient purification of mitochondria. Cells were transfected with Snn-FLAG-pcDNA3.1, incubated for 24 h and then the P2 fraction was isolated. Next, organelles within the P2 fraction were density-separated using a self-forming Percoll gradient. A, Western blots analyzed for the mitochondrial marker anti-GRP-75 (HSP-70), and anti-FLAG. Lanes: L, NIH-3T3 cell lysate; 1, top fraction from Percoll gradient; 2, dense band that had migrated 40% through the Percoll gradient, corresponding to mitochondria; 3, dense membrane collected at bottom of Percoll gradient. Note that immunoreactivity for the mitochondrial marker GRP-75 and Snn-FLAG was present only in the cell lysate and mitochondrial lanes. B, corresponds to Western blots verifying the purity of the Percoll purified mitochondria. Lanes: controls for total cell lysate from nontransfected cells (lanes 1 and 2) and Snn-FLAG-transfected cells (lanes 3 and 4); Percoll-purified mitochondria from nontransfected cells (lanes 5 and 6) and Snn-FLAG-transfected cells (lanes 7 and 8). Organelle markers are GRP-75 for mitochondria, GRP-78 for endoplasmic reticulum, α-spectrin for cytoskeleton, and Elk-1 for nucleus. C, quantitation of immunoreactivity in Western blots of organelle markers. Four lanes representing total cell lysate and mitochondrial samples were grouped and the average taken. Gray bars represent the average pixel value for total lysate conditions, and the black bars represent the average pixel value for the mitochondrial samples ± S.E.M.

pended in lysis buffer (described above). The BCA protein assay was performed to obtain protein concentrations. An equal amount of protein was added to Nu-PAGE laurel dodecyl sulfate sample buffer containing β-mercaptoethanol. Samples were denatured at 37°C for 10 min. Proteins were separated on Nu-PAGE precast polyacrylamide gels (SDS-PAGE; Invitrogen) and transferred to nitrocellulose membrane (Bio-Rad, Hercules, CA). Nitrocellulose membranes were incubated at room temperature for 15 min in blocking solution containing Tris-buffered saline (TBS), 0.1% Tween 20 (EM Scientific, Gibbstown, NJ), and 5% nonfat dry milk. Membranes were incubated with primary antibody (1:1000 dilution in blocking solution) overnight at 4°C, followed by a 15-min wash in TBS with 0.1% Tween 20. Membranes were incubated with a HRP-conjugated secondary antibody (1:10,000 dilution) at room temperature for 1 h in blocking solution, then washed in TBS with 0.1% Tween 20 for 1 h. Membranes were visualized using enhanced chemiluminescence reagent (ECL; Amersham Biosciences, Piscataway, NJ), exposed to ECL film (Amersham Biosciences), and developed using an X-ray developer.

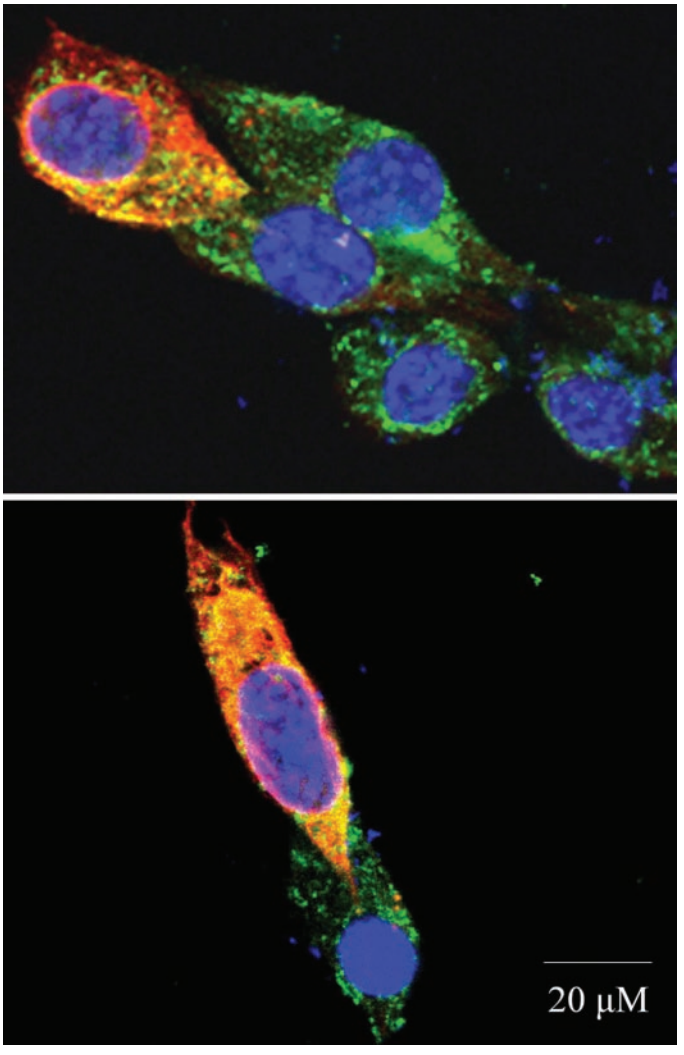

Fig. 4. Triple-label laser scanning confocal microscopy of Snn-FLAG-transfected NIH-3T3 cells. Cells were transfected with Snn-FLAG-pcDNA3.1, incubated for 24 h, then treated with anti-FLAG antibodies, anti-GRP-75 antibodies, and DAPI stain. Blue fluorophore (UV emission) corresponds to DAPI stained nuclei. Green fluorophore (FITC emission) corresponds to GRP-75 immunoreactivity. Note that all cells are stained with DAPI and show GRP-75 immunoreactivity. Red fluorophore (Texas Red emission) corresponds to Snn-FLAG immunoreactivity. Arrows indicate cells expressing Snn-FLAG. Micrographs were taken at 2500× magnification.

Cytotoxicity Measurement. Cells were plated into 12-well plates at a concentration of 3×10^4 cells per well and incubated at 37°C for 24 h. One microliter of LipofectAMINE 2000 and either 1.0 μg of GFP-FLAG-pcDNA3.1, Snn-FLAG-pcDNA3.1, or vehicle were incubated at 24°C for 20 min in 50 μl of Opti-MEM. This mixture was added to the cells and allowed to incubate at 37°C for 20 h. TMT (0.2 or 1.0 μM) or DMT (1.0 or 5.0 μM) was then added. Cells were incubated at 37°C for 24 h. Media was aspirated and cells were trypsinized and resuspended in 1.0 ml of media. Cells (100 μl) were added to 10 μl of 0.4% trypan blue. Viable and nonviable cells were then counted using a hemocytometer.

Results

Snn-FLAG Expression in NIH-3T3 Mouse Fibroblasts. Snn was engineered with an N-terminal FLAG epitope and subcloned into the pcDNA3.1 vector. The FLAG-tag antibodies were then used to detect Snn-FLAG expression. GFP was subcloned into the pcDNA3.1 vector with the addition of the FLAG-tag. The GFP-FLAG-pcDNA3.1 construct was used as an expression control on Western blot to verify relative levels Snn expression in NIH-3T3 cells (Fig. 1A). Given the transfection efficiencies of 25 to 30%, the extent of sensitization in these experiments may be masked, in part, by the presence of nontransfected cells. Laser-scanning confocal microscopy of Snn-FLAG-pcDNA3.1 and GFP-FLAG-pcDNA3.1 transfected NIH-3T3 cells indicate the relative levels of expression of both constructs (Fig. 1B).

Snn-FLAG Localizes to the Mitochondria. We initially performed subcellular fractionation using differential centrifugation to determine the organelle(s) to which Snn localizes. Characterization of the content of each of the fractions was based on protocol described by Graham (1982). Western blots were performed to analyze the presence of Snn in the different fractions. Only a minimal amount of Snn-FLAG immunoreactivity was found in the P1 fraction (nuclei and

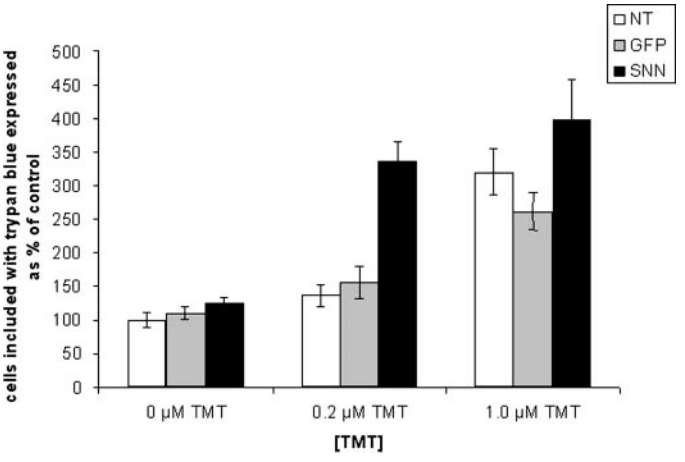

Fig. 5. TMT-induced cytotoxicity in Snn-FLAG-pcDNA3.1 transfected NIH-3T3 cells. Cells were transfected with Snn-FLAG-pcDNA3.1, incubated for 20 h, and then treated with either 0.2 or 1.0 μM DMT or no TMT, and incubated for 24 h. Cells were harvested and the number of nonviable cells quantitated using the trypan blue inclusion method. Denotation refers to: NT, nontransfection; GFP, GFP-FLAG-pcDNA3.1 transfection; SNN, Snn-FLAG-pcDNA3.1 transfection. After treatment with 0.2 μM TMT, the Snn-overexpressing cells exhibited significantly increased cytotoxicity compared with GFP-transfected or nontransfected controls (Student's t test; $p < 0.01$). After treatment with 1.0 μM TMT, cytotoxicity was increased in all groups, compared with untreated controls (Student's t test, $p < 0.01$). Data are shown as percentage of control; mean values ± S.E.M.

heavy mitochondria), indicating that Snn is most likely not found in the nucleus or nuclear membrane (Fig. 2). Furthermore, only a small amount of Snn-FLAG immunoreactivity was found in the cytosolic (S3) fraction, which may represent Snn in membrane that was not removed from the cytosol during the centrifugation process. Presence of Snn in the S3 fraction may also represent protein being trafficked to some membrane structure. A majority of Snn was found in the P2 (mitochondria, endoplasmic reticulum, peroxisomes) and P3 fractions (total membranes), at all times tested (20- and 24-h times shown). Differences between the amount of Snn in the P2 or P3 fractions over a range of times was tested. No significant changes were observed in the amount of Snn present in the P2 or P3 fractions at any time tested (data not shown).

To determine whether Snn specifically localized to the mitochondria, further purification of the P2 pellet was performed. First, to maintain a higher level of mitochondrial integrity, acquisition of the P2 pellet was modified using differentially prepared homogenization and Percoll gradient buffers, and plasma membrane was disrupted using a Dounce homogenizer. This method resulted in disruption of approximately 75% of cells, as verified through trypan blue inclusion. After the separation of the P2 fraction, a self-resolving Percoll gradient was used to separate intact mitochondria from endoplasmic reticulum and peroxisomes based on organelle density. Western blot examination of three of the Percoll fractions revealed the presence of Snn in the second fraction, indicated by anti-FLAG immunoreactivity (Fig. 3A). The presence of mitochondria in the second fraction was confirmed by immunoreactivity of glucose regulatory protein-75 (GRP-75), also known as mitochondrial-specific 70-kDa heat shock protein (HSP-70).

Verification of mitochondrial purity in the second Percoll gradient fraction was accomplished by screening for the presence of protein markers for other organelles that might contaminate the mitochondrial fraction (Fig. 3B). Minimal contamination was noted from nucleus (anti-Elk-1), endoplasmic reticulum (anti-GRP-78), and cytoskeleton (anti-α-spectrin). This indicates that Snn-FLAG immunoreactivity in the second Percoll gradient fraction represented the presence of Snn in mitochondria. Quantitation of the presence of each organelle marker was performed. The average pixel density found in total cell lysate was compared with the pixel density observed in the purified mitochondria (Fig. 3C).

Immunofluorescent laser scanning confocal microscopy was performed to visualize the colocalization of Snn and the mitochondrial protein GRP-75 (Fig. 4). Snn-FLAG-pcDNA3.1 transfected cells can be visualized adjacent to nontransfected cells. All cells within the selected fields show immunofluo-

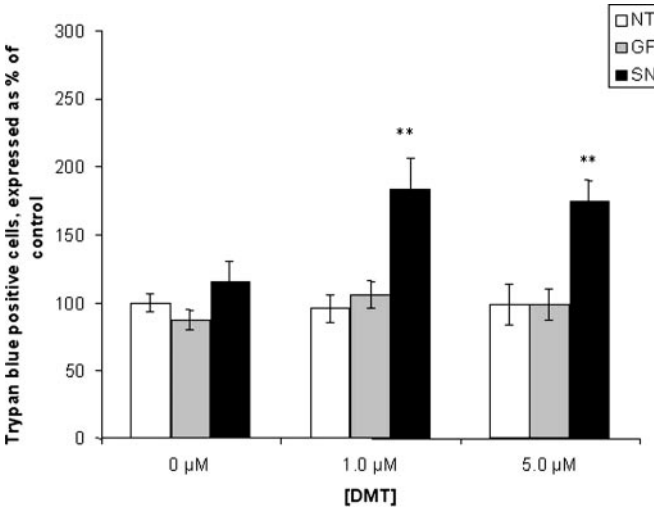

Fig. 6. DMT-induced cytotoxicity in Snn-FLAG-pcDNA3.1-transfected NIH-3T3 cells. Cells were transfected with Snn-FLAG-pcDNA3.1, incubated for 20 h, and then treated with either 1.0 or 5.0 μM DMT or no DMT, and incubated for 24 h. Cells were harvested and the number of nonviable cells quantitated using the trypan blue inclusion method. Denotation refers to: NT, nontransfection; GFP, GFP-FLAG-pcDNA3.1 transfection; SNN, Snn-FLAG-pcDNA3.1 transfection. At both concentrations of DMT, Snn overexpression significantly increased the number of cells included with trypan blue, compared with GFP-transfected and nontransfected controls (Student's t test, $p < 0.01$). Data are shown as percentage of control; mean values ± S.E.M.

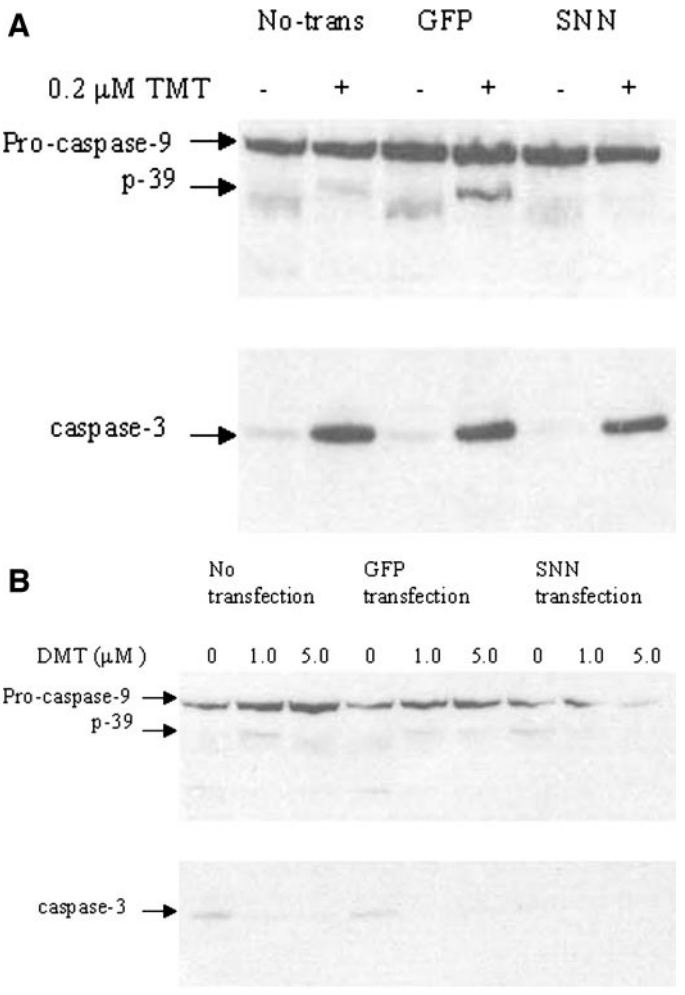

Fig. 7. Caspase-9 and -3 activity after TMT and DMT treatment. Cells were transfected with Snn-FLAG-pcDNA3.1, GFP-FLAG-pcDNA3.1, or no DNA and incubated for 20 h. TMT (0.2 μM) or DMT (1.0 and 5.0 μM) was then added and incubated for 24 h. Cells were lysed and 50 μg of total protein analyzed on Western blots. A, Western blots of TMT-treated cells; immunoreactivity for activated caspase-3 was visible in all transfection conditions when treated with 0.2 μM TMT. Procaspase-9 immunoreactivity was visible in all conditions. A small amount of activated (p39) caspase-9 immunoreactivity was present in nontransfected and GFP-transfected cells treated with 0.2 μM TMT. No immunoreactivity for activated (p39) caspase-9 was present in Snn-transfected cells ± TMT. B, Western blots of DMT-treated cells. Immunoreactivity for activated caspase-3 was not visible in any condition. Immunoreactivity for procaspase-9 was visible in all conditions; however, activated (p39) caspase-9 immunoreactivity was absent in all conditions.

rescence for GRP-75 (green fluorophore) and positive DAPI staining (blue fluorophore). The Snn-FLAG-pcDNA3.1 transfected cells show immunofluorescence for Snn (red fluorophore). The colocalization of Snn and GRP-75 is indicated by the presence of yellow overlay. The presence of a pool of Snn that does not colocalize with GRP-75 most probably represents Snn that localizes to other intracellular compartments. This is consistent with the presence of Snn in several fractions in the differential centrifugation experiments.

Stannin Overexpression Sensitizes NIH-3T3 Cells to TMT and DMT Toxicity. NIH-3T3 fibroblasts are resistant to TMT-induced toxicity; furthermore, they express very low levels of Snn, compared with other immortalized cell lines (Thompson et al., 1996). Thus, NIH-3T3 cells were chosen as a model to test the conference of TMT sensitivity by Snn overexpression. After treatment with 0.2 μM TMT for 24 h, significantly increased trypan blue inclusion was noted in Snn-FLAG-pcDNA3.1 transfected cells, compared with GFP-FLAG-pcDNA3.1-transfected and nontransfected control cells (Fig. 5). No differences between groups were revealed in the 1.0 μM TMT-treated conditions.

Recent research has shown that Snn may directly dealkylate TMT and retain association with the subsequent product, DMT (Buck et al., 2003). This led us to examine Snn's possible role in mediating DMT toxicity. Initial screening of high- and low-Snn-expressing cells (HEK-293 and NIH-3T3 cells, respectively) revealed that NIH-3T3 cells exhibited resistance to DMT-induced cytotoxicity compared with HEK-293 cells (data not shown). Transfection of NIH-3T3 cells with Snn-FLAG-pcDNA3.1 conveyed significant sensitization to cytotoxicity at both 1.0 and 5.0 μM DMT (Fig. 6). On the other hand, transfection of GFP-FLAG-pcDNA3.1 did not sensitize cells to DMT-induced toxicity, compared with nontransfected controls. This indicates that Snn overexpression can confer increased sensitivity to DMT-induced as well as TMT-induced cytotoxicity.

Snn Overexpression Does Not Increase Caspase Activation after TMT and DMT Treatment. TMT administration elicits cellular responses that are indicative of both necrotic and apoptotic cell death. To determine whether the increased cytotoxicity was mediated by caspases, we analyzed the cellular content of activated caspase-9 and -3 after TMT and DMT treatment. NIH-3T3 fibroblasts were transfected with Snn-FLAG-pcDNA3.1, GFP-FLAG-pcDNA3.1, or no DNA and treated with TMT (0.2 μM) or DMT (1.0 or 5.0 μM). The 1.0 μM treatment of TMT elicited cytotoxicity in all transfection conditions; therefore, only the 0.2 μM concentration was used to analyze differential caspase activation. Western blot analysis of GFP and nontransfection conditions after TMT treatment revealed a small amount of active caspase-9 immunoreactivity (Fig. 7a). Conversely, no active caspase-9 immunoreactivity was found in the Snn-transfection condition after TMT treatment. Western blot analysis for active caspase-3 revealed that all TMT treatments elicited caspase-3 activation under all transfection conditions. Furthermore, no differences were noted in active caspase-3

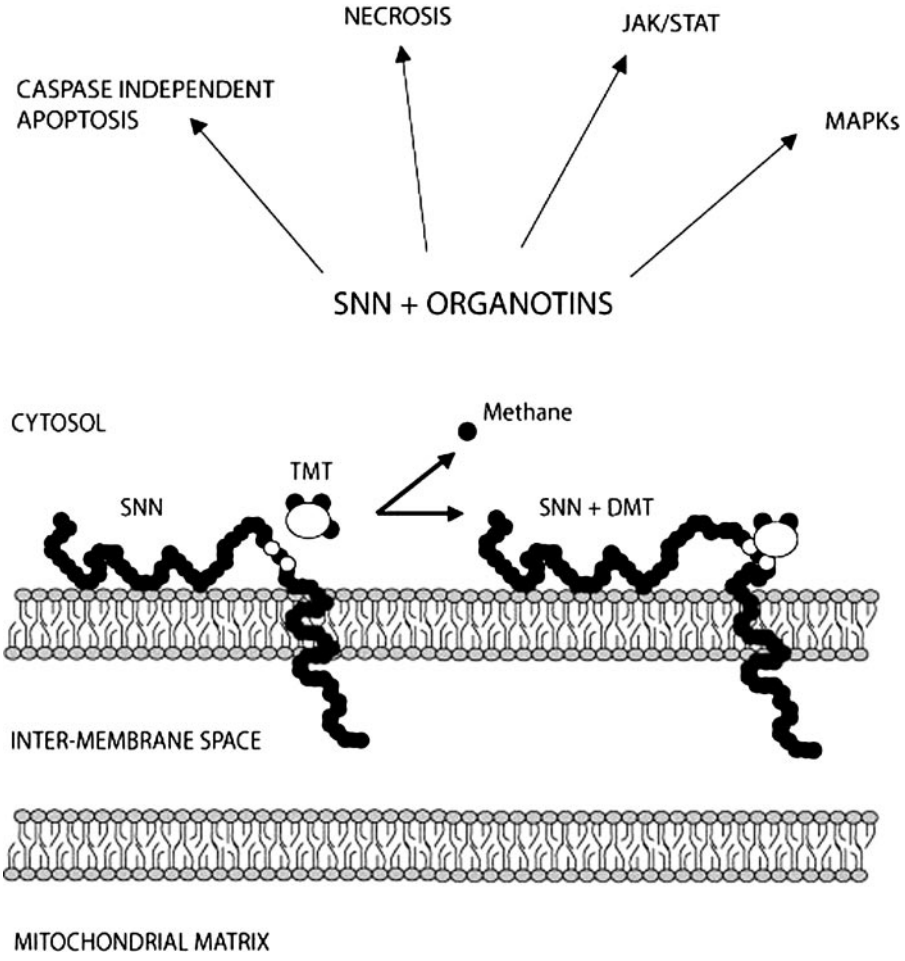

Fig. 8. Model of proposed role for interaction between stannin and methyltins. Shown is a model of the possible localization of Snn in the outer mitochondrial membrane. In this orientation, the vicinal dithiol (residues 32 and 34) provides a possible binding domain for organotins. Shown is the proposed interaction of Snn with TMT and its subsequent dealkylation. The localization of Snn to mitochondria provides a mechanistic link to the mitochondrial toxicity observed after TMT exposure. The direct interaction of stannin with TMT and DMT is based on data from Buck et al. (2003).

immunoreactivity between Snn and control conditions, ± TMT treatment. Western blot analysis of DMT-treated cells revealed that the 1.0 and 5.0 μM treatments did not result in significant activation of caspase-3 or caspase-9 in any of the transfection conditions. This is indicated by the lack of immunoreactivity for active caspase-3 and active (p39) caspase-9 (Fig. 7b). These data indicate that Snn overexpression in NIH-3T3 cells does not preactivate caspase cascades. Furthermore, caspase cascades are not differentially activated after TMT and DMT treatment in Snn-transfected cells compared with control conditions.

Discussion

Our results demonstrate that a significant portion of Snn localizes to mitochondria after transfection of NIH-3T3 fibroblasts. Because our model system employs transient transfection and expression of Snn is under the control of a strong cytomegaloviral promoter, the levels of Snn may exceed those normally encountered. It is likely that Snn is also present in endoplasmic reticulum. Transcript/Translation summaries from Sanger Institute protein analyses indicate that Snn may also contain a secretion signal (Snn; http://www.ensembl.org). Thus, Snn may localize to endoplasmic reticulum and Golgi apparatus during processing. This is consistent with the current differential centrifugation data showing Snn localized to multiple compartments. These results show that isolated and purified mitochondria contained Snn within that compartment.

The mechanism by which Snn is targeted to the mitochondrial membrane is unclear. Sequence analysis of Snn does not reveal the existence of a known mitochondrial localization signal; however, this is not uncommon. Tail-anchored proteins are known to localize to membrane surfaces that face the cytosol, including the outer mitochondrial membrane, although they do not contain a traditional mitochondrial localization signal (Borgese et al., 2003; Habib et al., 2003). Recent evidence has also shown that proteins may translocate to the mitochondria after alterations in their phosphorylation status (Bijur and Jope, 2003; Robin et al., 2003). Analysis of Snn's amino acid sequence reveals multiple residues that have high probabilities of phosphorylation (data not shown), which may provide a possible mechanism for mitochondrial targeting.

The high level of sequence conservation of Snn across vertebrates, and the temporal and spatial patterns of expression suggest an important function for this protein. However, no homologies have been found for Snn, nor does Snn contain any domains that may provide insight into a possible intracellular role. For these reasons, research has concentrated on Snn's role in mediation of organotin toxicity. Snn transfection sensitized cells that normally show resistance to TMT- and DMT-induced cytotoxicity. Furthermore, we have shown that DMT is only toxic to NIH-3T3 cells when they overexpress Snn. It is possible that Snn is a common factor required for organotin toxicity, with TMT as the most potent toxicant.

Comparative toxicity studies after TMT administration in vivo and in vitro show that DMT is less toxic than TMT (Mushak et al., 1982; Komulainen and Bondy, 1987). Our results indicated that DMT did not elicit cytotoxicity when administered to NIH-3T3 cells, or NIH-3T3 cells transfected with GFP. NIH-3T3 cells that were transfected with Snn, however, exhibited marked sensitivity to DMT. This indicates that DMT may interact with Snn to elicit cytotoxicity. Although Snn overexpression conferred DMT sensitivity to NIH-3T3 cells, TMT treatment produced a more potent cytotoxicity. This may indicate that the interaction of Snn with TMT and subsequent dealkylation of TMT to DMT plays an integral role in the molecular basis of TMT-induced cytotoxicity. Oligonucleotide-mediated knockdown of Snn expression in vitro protected primary neurons in culture from TMT-induced cytotoxicity (Thompson et al., 1996). Together, this evidence indicates that inhibition of the TMT-Snn interaction may block TMT-induced cell death.

Morphological and molecular evidence after TMT exposure has indicated that TMT treatment can result in apoptotic and necrotic cell death, alluding to multiple mechanisms of toxicity (Brown et al., 1979; Bruccoleri et al., 1998; Gunasekar et al., 2001; Geloso et al., 2002; Jenkins and Barone, 2004). TMT treatment of PC-12 cells in vitro results in caspase-3 and -9 activation (Jenkins and Barone, 2004). Herein, we show corroborating increases in caspase-3 and -9 activation after TMT treatment of NIH-3T3 cells. Snn overexpression did not preactivate caspase cascades, nor did it amplify caspase activity after TMT treatment. DMT-treated cells exhibited a total lack of caspase activation under all conditions. This suggests that caspase activation is not a common phenomenon after treatment with organotins.

Significant increases in trypan blue inclusion occurred only in Snn-overexpressing cells treated with TMT and DMT. TMT-elicited increase in caspase activity and cytotoxicity are likely to occur via separate mechanisms in cells transfected with Snn. Furthermore, TMT-induced caspase-9 activation was attenuated by overexpression of Snn; this may indicate that Snn overexpression drives a form of cell death that is not dependent upon mitochondrial-mediated activation of caspase-9.

Recent reports indicated that p38/mitogen-activated protein kinase inhibitors can effectively block TMT-induced cytotoxicity in vitro (Jenkins and Barone, 2004), providing another possible mechanism by which Snn may mediate organotin-induced cytotoxicity. These experiments, as well as the current data, examined organotin-induced cytotoxicity in vitro. The molecular mechanisms seen in transfected cells in vitro may not reflect the toxicological effects observed after TMT administration in vivo. Additional research is required to elucidate the molecular basis of TMT-induced cytotoxicity using both in vivo and in vitro models.

In conclusion, these data show that overexpression of Snn can confer sensitivity to two organotins. Moreover, given the mitochondrial localization and the putative role of Snn as an organotin-binding protein, we suggest a possible mechanism whereby TMT and DMT can bind to and disrupt Snn (Fig. 8). The Snn/organotin interaction leads to cellular toxicity that may be mediated by multiple mechanisms, including Janus tyrosine kinase/signal transducer and activator of transcription, mitogen-activated protein kinase, caspase-independent apoptotic, or necrotic pathways. Further work will be needed to determine the normal function for this highly conserved protein.

References

Aschner M and Aschner JL (1992) Cellular and molecular effects of trimethyltin and triethyltin: relevance to organotin neurotoxicity. *Neurosci Biobehav Rev* **16:**427–435.

Balaban CD, O'Callaghan JP, and Billingsley ML (1988) Trimethyltin-induced neu-

ronal damage in the rat brain: comparative studies using silver degeneration stains, immunocytochemistry and immunoassay for neuronotypic and gliotypic proteins. *Neuroscience* **26:**337–361.
Bijur GN and Jope RS (2003) Rapid accumulation of Akt in mitochondria following phosphatidylinositol 3-kinase activation. *J Neurochem* **87:**1427–1435.
Borgese N, Colombo S, and Pedrazzini E (2003) The tale of tail-anchored proteins: coming from the cytosol and looking for a membrane. *J Cell Biol* **161:**1013–1019.
Boyer IJ (1989) Toxicity of dibutyltin, tributyltin and other organotin compounds to humans and to experimental animals. *Toxicology* **55:**253–298.
Braman RS and Tompkins MA (1979) Separation and determination of nanogram amounts of inorganic tin and methyltin compounds in the environment. *Anal Chem* **51:**12–19.
Brown AW, Aldridge WN, Street BW, and Verschoyle RD (1979) The behavioral and neuropathologic sequelae of intoxication by trimethyltin compounds in the rat. *Am J Pathol* **97:**59–82.
Bruccoleri A, Brown H, and Harry GJ (1998) Cellular localization and temporal elevation of tumor necrosis factor-alpha, interleukin-1 alpha and transforming growth factor-beta 1 mRNA in hippocampal injury response induced by trimethyltin. *J Neurochem* **71:**1577–1587.
Buck B, Mascioni A, Que LJ, and Veglia G (2003) Dealkylation of organotin compounds by biological dithiols: toward the chemistry of organotin toxicity. *J Am Chem Soc* **125:**13316–13317.
Dejneka NS, Patanow CM, Polavarapu R, Toggas SM, Krady JK, and Billingsley ML (1997) Localization and characterization of stannin: relationship to cellular sensitivity to organotin compounds. *Neurochem Int* **31:**801–815.
Dyer RS, Walsh TJ, Wonderlin WF, and Bercegeay M (1982) The trimethyltin syndrome in rats. *Neurobehav Toxicol Teratol* **4:**127–133.
Feldman GR, White RF, and Ikechukwu EI (1993) Trimethyltin encephalopathy. *Arch Neurol* **50:**1320–1324.
Geloso MC, Vercelli A, Corvino V, Repici M, Boca M, Haglid K, Zelano G, and Michetti F (2002) Cyclooxygenase-2 and caspase 3 expression in trimethyltin-induced apoptosis in the mouse hippocampus. *Exp Neurol* **175:**152–160.
Graham J (1982) Isolation of subcellular organelles and membranes, in *Centrifugation, A Practical Approach* (Rickwood D ed) pp 161–182, IRL Press, Washington, DC.
Gunasekar P, Li L, Prabhakaran K, Eybl V, Borowitz JL, and Isom GE (2001) Mechanisms of the apoptotic and necrotic actions of trimethyltin in cerebellar granule cells. *Toxicol Sci* **64:**83–89.
Habib SJ, Vasiljev A, Neupert W, and Rapaport D (2003) Multiple functions of tail-anchor domains of mitochondrial outer membrane proteins. *FEBS Lett* **555:**511–515.
Jenkins SM and Barone S (2004) The neurotoxicant trimethyltin induces apoptosis via caspase activation, p38 protein kinase and oxidative stress in PC12 cells. *Toxicol Lett* **147:**63–72.
Komulainen H and Bondy SC (1987) Increased free intrasynaptosomal Ca^{2+} by neurotoxic organometals: distinctive mechanisms. *Toxicol Appl Pharmacol* **88:**77–86.
Krady JK, Oyler GA, Balaban CD, and Billingsley ML (1990) Use of avidin-biotin subtractive hybridization to characterize mRNA common to neurons destroyed by the selective neurotoxicant trimethyltin. *Brain Res Mol Brain Res* **7:**287–297.
LeBel CP, Ali SF, McKee M, and Bondy SC (1990) Organometal-induced increases in oxygen reactive species: the potential of 2′,7′-dichlorofluorescin diacetate as an index of neurotoxic damage. *Toxicol Appl Pharmacol* **104:**17–24.
Mushak P, Krigman MR, and Mailman RB (1982) Comparative organotin toxicity in the developing rat: somatic and morphological changes and relationship to accumulation of total tin. *Neurobehav Toxicol Teratol* **4:**209–215.
Noland EA, McCauley PT, and Bull RJ (1983) Dimethyltin dichloride: investigations into its gastrointestinal absorption and transplacental transfer. *J Toxicol Environ Health* **12:**89–98.
Philbert MA, Billingsley ML, and Reuhl KR (2000) Mechanisms of injury in the central nervous system. *Toxicol Pathol* **28:**43–53.
Robin MA, Prabu SK, Raza H, Anandatheerthavarada HK, and Avadhani NG (2003) Phosphorylation enhances mitochondrial targeting of GSTA4-4 through increased affinity for binding to cytoplasmic Hsp70. *J Biol Chem* **278:**18960–70.
Ross WD, Emmett EA, Steiner J, and Tureen R (1981) Neurotoxic effects of occupational exposure to organotins. *Am J Psychiatry* **138:**1092–1095.
Sadiki A and Williams DT (1996) Speciation of organotin and organolead compounds in drinking water by gas chromatography–atomic emission spectrometry. *Chemosphere* **32:**1983–1992.
Snoeij NJ, Penninks AH, and Seinen W (1987) Biological activity of organotin compounds—an overview. *Environ Res* **44:**335–353.
Snoeij NJ, van Iersel AA, Penninks AH, and Seinen W (1985) Toxicity of triorganotin compounds: comparative in vivo studies with a series of trialkyltin compounds and triphenyltin chloride in male rats. *Toxicol Appl Pharmacol* **81:**274–286.
Stine KE, Reiter LW, and Lemasters JJ (1988) Alkyltin inhibition of ATPase activities in tissue homogenates and subcellular fractions from adult and neonatal rats. *Toxicol Appl Pharmacol* **94:**394–406.
Thompson TA, Lewis JM, Dejneka NS, Severs WB, Polavarapu R, and Billingsley ML (1996) Induction of apoptosis by organotin compounds in vitro: neuronal protection with antisense oligonucleotides directed against stannin. *J Pharmacol Exp Ther* **276:**1201–1216.
Toggas SM, Krady JK, and Billingsley ML (1992) Molecular neurotoxicology of trimethyltin: identification of stannin, a novel protein expressed in trimethyltin-sensitive cells. *Mol Pharmacol* **42:**44–56.

Address correspondence to: Dr. Jong K. Yun, H078 Department of Pharmacology, 500 University Dr., Penn. State College of Medicine, Hershey, PA 17033. E-mail: jky1@psu.edu